Picosecond dynamics of barrier crossing in solution: A study of the conformational change of excited state 1,1′-binaphthyl

David P. Millar[a] and Kenneth B. Eisenthal
Department of Chemistry, Columbia University, New York, New York 10027

(Received 22 April 1985; accepted 25 July 1985)

The rates of optically induced conformational changes of excited state 1,1′-binaphthyl in a series of alcohol solvents were measured by a picosecond laser technique. Excellent agreement with experiment is found for the Kramers model for both the intermediate and high friction regimes using a frequency independent friction coefficient evaluated from classical hydrodynamics. This is the first observation of Kramers behavior in the intermediate friction regime and indicates that deviations from Kramers behavior is not a universal phenomenon in the conformational dynamics of flexible molecules in solution. It also emphasizes the possibility that the observed deviations from the Kramers model can be due to effects other than non-Markovian friction.

I. INTRODUCTION

The conformational and isomerization dynamics of flexible molecules in solution have been the subject of recent interest as a test of solution phase reaction theories. These processes can be considered as unimolecular reactions which involve the passage across a potential barrier from "reactant" to "product" configurations. The effect of the solvent on the barrier crossing dynamics has been the subject of considerable experimental[1–8] and theoretical[9–21] attention in recent years. Following the early work of Kramers,[22] several theoretical treatments have employed a one-dimensional Langevin equation to model the dynamics.[9–11] In this approach the solvent imposes a frictional drag force and a random fluctuating force on the solute motion governed by the intramolecular potential. The Kramers model was recently extended to include non-Markovian solvent response,[12,13] multidimensional systems,[14,15] and the entire friction range.[13,16] Another theoretical approach has been the development of stochastic collisional models, such as the BGK model,[17–20] in which the solvent affects the solute motion via impulsive collisions. Molecular dynamics and stochastic calculations of isomerization dynamics have also been performed.[21]

The qualitative picture of the solvent effect on the barrier crossing dynamics is essentially the same in all these models. For weak coupling of the solute motion to the solvent degrees of freedom (low friction or collision frequency) the barrier crossing rate increases linearly with coupling, since the rate limiting step is excitation of the solute to the barrier region. For strong coupling, the rate decreases with increasing coupling due to diffusional recrossings of the barrier. In the intermediate regime the rate attains its maximum value. An upper limit to this maximum rate is provided by classical transition state theory (TST), since the assumptions of equilibrium in the barrier region and a one-way flux across the barrier, which are inherent in TST and lead to the maximum possible crossing rate, can never be exactly satisfied in solution. One of the differences between the frictional and collisional models is the extent to which these assumptions are violated and hence how closely the crossing rate in the intermediate regime approaches to TST value. The frictional model generally leads to a closer attainment of the TST limit than the collisional models.[18]

The comparison of the theoretical models with the experimental data available to date has not been wholly successful. Several groups have studied the viscosity dependence of the conformational or isomerization dynamics of systems in which bulky molecular groups rotate about single or double bonds.[1–7] In all these studies the barrier crossing rate was observed to decrease monotonically as the viscosity increased, which is characteristic of the strong coupling regime. Since it seemed reasonable that the solute–solvent coupling in these systems was frictional, these data were compared with Kramers solution of the Langevin model in the strong coupling limit ("Kramers equation"). For diphenylbutadiene[2] and *trans*-stilbene[6] in alkane solvents, and the dye DODCI in alcohol solvents,[3] the data showed significant deviation from Kramers equation. One explanation for this behavior is that the solvent friction is frequency dependent, which is expected to cause deviations from Kramers equation for molecules with very sharply curved barriers to isomerization.[12,23] This view was apparently confirmed by the observation that for diphenylbutadiene and stilbene in alcohol solvents, where the barrier curvature was smaller relative to the alkane solvents, the data were in good agreement with Kramers equation in the Smoluchowski (high viscosity) limit.[4,5,7] However, for stilbene in alkane solvents[6] it was found that agreement with Kramers equation in the Smoluchowski limit could be obtained by "stiffening" the stilbene—that is, restricting the conformational degrees of freedom of the molecule by incorporating the phenyl groups into a fused ring system.[6] Although this agreement in the Smoluchowski limit could be due, in part, to a flattening of the barrier, the reduction in the isomerization related conformational degrees of freedom could also be pertinent. The question of whether the observed deviations from Kramers' behavior are due to frequency dependent solvent friction effects, the participation of more than one conformational coordinate, or other factors, requires closer examination.

In this paper we report measurements of the rate of opti-

---

[a] Present Address: Department of Physical Chemistry, The University of Sydney, Sydney, N. S. W. 2006, Australia.

0021-9606/85/225076-08$02.10

cally induced conformational changes in the first excited singlet state of 1,1′-binaphthyl in a series of alcohol solvent. The conformational change involves the reaction of the two naphthyl groups about the connecting single bond (see Fig. 1) and, having a single coordinate in the structural change, should approach a one-dimensional system more closely than diphenylbutadiene, *trans*-stilbene, or DODCI. In view of the possibility that multidimensional effects may cause deviations from Kramers equation, it is clearly of interest to investigate the conformational dynamics of 1,1′-BN. Actually, the conformational dynamics of 1,1′-BN have been investigated in an earlier study[1] by us and later compared with Kramers equation.[9] However, in that study measurements were made at only three viscosities and the theoretical comparison required the use of two adjustable parameters. In view of the relevance of 1,1′-BN to the questions raised above, it is important to provide a more stringent comparison of *both* the Kramers model and the frequency dependent friction model with data spanning a wider range of viscosity. This is the purpose of the present paper.

The spectroscopic data on 1,1′-BN[24–27] suggest that the S_1 state is characterized by a double well potential surface of the form shown in Fig. 2. The two minima are characterized by different dihedral angles between the naphthyl groups. The existence of the barrier was revealed by the temperature dependence of the solution phase fluorescence spectrum.[25] This form of the potential surface is also predicted from electronic structure calculations,[28,29] which show that there is a crossing from an A symmetry excited state to a lower energy B state as the dihedral angle is changed. Both the calculations and the spectroscopic evidence suggest that the minima are separated by about 40°.[27–29]

In a rigid solution at low temperature, fluorescence is only observed from the higher energy excited conformer (conformer 1) or, in those cases where both conformers exist in the ground state,[27] from both excited conformers. However, in fluid solution fluorescence is only observed from the lower energy excited conformer (conformer 2).[25,26] This suggests that a rapid relaxation from conformer 1 to conformer 2, achieved by rotation of the naphthyl groups about the connecting bond, occurs in the excited state in fluid solution. It is this conformational change that we consider in this paper.

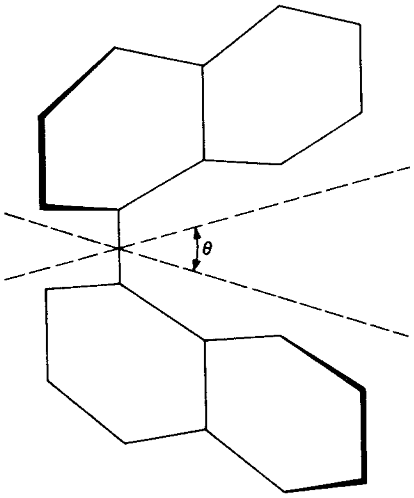

FIG. 1. 1,1′-binaphthyl. The dihedral angle θ involved in the conformational change is indicated.

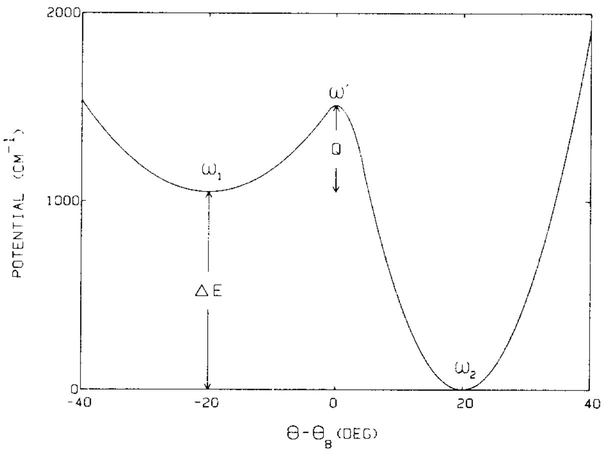

FIG. 2. A piecewise parabolic representation of the S_1 excited state potential function of the form given by Eq. (11). The dihedral angle is measured relative to the barrier configuration θ_b. The frequency of the upper well ω_1, the lower well ω_2, and the barrier ω' are indicated. The barrier height Q and energy difference ΔE are also indicated. The values $\omega_1 = 5.7\ \mathrm{ps}^{-1}$, $\omega_2 = 11.3\ \mathrm{ps}^{-1}$, $\omega' = 21.5\ \mathrm{ps}^{-1}$, $Q = 460\ \mathrm{cm}^{-1}$, and $\Delta E = 1050\ \mathrm{cm}^{-1}$ were used to calculate the potential shown here. See Sec. IV B for details.

We have used a picosecond pump–probe technique to measure the rate of appearance of conformer 2 following excitation of conformer 1. This provides the rate of barrier crossing on the excited state potential surface. An ultraviolet pump pulse excites molecules onto the S_1 surface and a time delayed visible probe pulse monitors an $S_1 \rightarrow S_n$ transient absorption due to conformer 2. The experimental details are described in Sec. II. In Sec. III we briefly review the Kramers and frequency dependent friction models. In Sec. IV we present our results of the barrier crossing rate of 1,1′-BN in a series of alcohol solvents spanning the viscosity range 1.2–9 cP and then compare them with the two theoretical models.

II. EXPERIMENTAL

The experimental apparatus is shown in Fig. 3. A high repetition rate (82 MHz) synchronously mode-locked rhodamine 6G dye laser (Spectra Physics model 365) was used as the source of picosecond pulses. The laser wavelength was 600 nm and the pulse duration was 4 ps, as inferred from second harmonic autocorrelation measurements corrected for the effect of pulse substructure.[30] The laser output was split into a strong beam and a weak beam. The strong beam was focused into a 1 mm thick crystal of $LiIO_3$ to generate the second harmonic at 300 nm. The weak beam passed along a variable delay path before recombining with the UV beam. These "pump" (UV) and "probe" (red) beams were focused into a 5×10^{-3} M solution of 1,1′-BN contained in a 1 mm path length cuvette. The energy of a single pump pulse at the sample was 6 pJ. The pump and probe polarization directions were orthogonal, since this configuration was most sensitive to the transient absorption associated with the conformational change.[1] The relative arrival time of pump and probe pulses at the sample was varied by a stepper motor

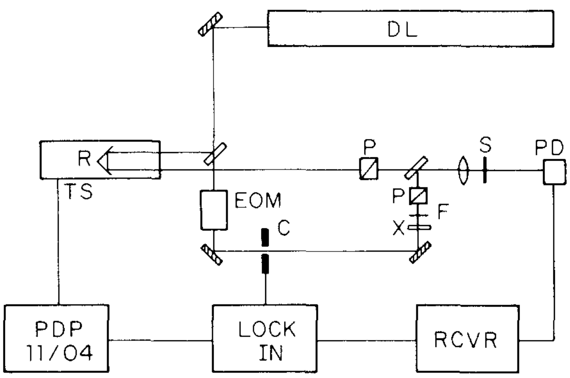

FIG. 3. Diagram of the experimental apparatus. DL: synchronously mode-locked dye laser, EOM: electro-optic modulator, C: chopper, TS: translation stage, X: $LiIO_3$ frequency doubling crystal, F: UV pass filter, P: polarizers, S: sample, PD: photodiode, RCVR: communication receiver.

driven translation stage. The transmitted probe beam passed to a photodiode which was connected to the antenna input of a communications receiver (Drake R7A). The radio output was connected to a lock-in amplifier (PAR model 142).

Since relatively few excited molecules were produced by the low energy pump pulse, the change in the probe beam intensity due to the $S_1 \rightarrow S_n$ transient absorption was very small. A sensitive detection technique was therefore required. The pump beam was intensity modulated at 14 MHz by an electro-optic modulator (Coherent model 28), driven by a radio transmitter (Drake TR7), and also at 400 Hz by a mechanical chopper. The resulting intensity modulation on the transmitted probe beam, due to transient absorption induced by the pump, was demodulated by the radio receiver and lock-in amplifier combination. The radio was operated in a linear response regime. This double modulation technique[31] allowed very small absorptions to be measured by taking advantage of the low noise characteristics of the synchronously mode-locked dye laser at megahertz frequencies. The lock-in amplifier was interfaced to a microcomputer (PDP 11/04) which also controlled the stepper motor driven translation stage. Various modes of data acquisition, multiple sweep averaging, graphics, and data analysis were performed on the computer.

Alcohol solvents were distilled prior to use and stored over drying agents. Measurements were performed at 18.5 °C.

III. THEORETICAL MODELS

A. The Kramers model

Kramers[22] employed a Langevin equation to describe the motion of a particle in a one-dimensional potential well subject to friction and fluctuating forces caused by interaction with the surrounding medium. The friction is considered to be Markovian—that is, the forces acting on the particle are uncorrelated. From the steady-state solution of the associate Fokker–Planck equation, Kramers found the rate at which particles escape from the well by crossing a potential barrier. The expression for the barrier crossing rate in the strong coupling regime is[22]

$$K = \omega(2\pi\omega')^{-1}[(\beta^2/4 + \omega'^2)^{1/2} - \beta/2]e^{-Q/kT}, \tag{1}$$

where Q is the height of the barrier, ω and ω' are frequencies associated with the second derivatives of the potential at the well and barrier, respectively, and β is the reduced friction coefficient. In the absence of hydrodynamic interactions between the two naphthyl groups this last quantity is given by[9]

$$\beta = \zeta_r / I, \tag{2}$$

where ζ_r is the friction coefficient for rotation of a single naphthyl group about the 1,1′ bond and I is the moment of inertia of a single naphthyl group. For a polyatomic molecule such as 1,1′-BN, Eq. (1) should be multiplied by the ratio $Z^{\neq}/Z'$. $Z^{\neq}$ is the partition function at the barrier configuration with the reaction coordinate removed and Z' is the corresponding quantity at the bottom of the reactant well. Since we are using a one-dimensional Kramers model the partition function ratio was taken as unity. The assumption of setting the ratio equal to one for the case of 1,1′-BN is valid provided there are no large frequency shifts in the vibrational modes. For the S_1 state of 1,1′-BN, the weakly interacting[28,39] naphthalene chromophores support this approximation. In the general case where there are frequency shifts, then the partition function ratio would simply scale the Kramers equation without modifying its frictional dependence.

To make comparison of Kramers equation with experimental data it is necessary to adopt a model which relates the friction coefficient to the shear viscosity of the solvent. The hydrodynamic model is frequently used in this regard. For 1,1′-BN the hydrodynamic model gives[32]

$$\zeta_r = 4\pi\eta_s d r^2, \tag{3}$$

where d is the radius of a naphthyl group approximated as a sphere, r is the radius of gyration and η_s is the shear viscosity of the solvent. A slip boundary condition is assumed in Eq. (3), which is appropriate for a nonpolar molecule such as 1,1′-BN.[33,34] It should be remarked that the use of hydrodynamics is an additional approximation that is not implicit in the Kramers model. It was used in all the previous comparisons with experimental data.[2–4,6,9] It is a reasonable starting point and we adopt it in our study also.

In the limit of sufficiently high viscosity, which is referred to as the Smoluchowski limit, Eq. (1) reduces to

$$K = \omega\omega'(2\pi\beta)^{-1}e^{-Q/kT}. \tag{4}$$

This simpler Smoluchowski equation is valid when $(2\omega^2 + \omega'^2)/\beta \ll 1$,[9] and describes the limiting situation where the barrier crossing dynamics are dominated by the effect of the solvent friction. Note that the barrier crossing rate is inversely proportional to the friction in this limit.

B. Frequency dependent friction model

Grote and Hynes[12] have obtained the escape rate for the Kramers model including non-Markovian solvent response. Their approach recognizes that for barrier crossing occurring on a sufficiently short time scale, which is the case on sharply curved barriers, the forces acting on the solute cannot be considered as uncorrelated. The situation can be described by a time and frequency dependent friction coefficient.

The barrier crossing rate in this model is[12]

$$K = \omega(2\pi\omega')^{-1}\lambda_r e^{-Q/kT}, \tag{5}$$

where λ_r is a reactive frequency found from the iterative solution to the equation

$$\lambda_r = \omega'^2/[\lambda_r + \zeta(\lambda_r)/I\,], \tag{6}$$

provided that $\lambda_r \leqslant \omega'$. $\zeta(\lambda_r)$ is the frequency dependent friction coefficient evaluated at the reactive frequency.

In order to implement the Grote–Hynes model the frequency dependence of the friction coefficient must be known. Unfortunately, very little is presently known about the frequency dependence. We have therefore adopted the model formulations used in previous work in this area.[6,23,35,36] It is to be emphasized that the use of a hydrodynamic model for the friction is not part of the Grote–Hynes model. Its introduction therefore complicates the experimental testing of the validity of the Grote–Hynes theory, since the hydrodynamic frequency dependent model can be incorrect and furthermore is likely to fail at very high frequencies or short times.[35–38] Recognizing these limits we nonetheless use the hydrodynamic model since it permits us to obtain a usable expression for the frequency dependent friction. For these reasons we take the friction coefficient to be the frequency dependent hydrodynamic friction appropriate to a sphere,[35,36]

$$\zeta_r(s) = 4\pi\eta_s(s) d r^2 X_2\ [2(X+1)P + (Y+1)R\,], \tag{7}$$

where

$$X = [sp/\eta_s(s)]^{1/2} d,$$
$$Y = s[C_s^2 + s\eta_1(s)/\rho]^{-1/2} d,$$
$$P = (3 + 3Y + Y^2)/\Delta,$$
$$R = [3 + 3X + X^2 + 0.5X^2(1 + X\,]/\Delta,$$
$$\Delta = 2X^2(3 + 3Y + Y^2) + Y^2(3 + 3X + X^2)$$
$$+ 1.5X^2(1 + X)(2 + 2Y + Y^2).$$

The quantities $\eta_s(s)$ and $\eta_1(s)$ are the frequency dependent solvent shear and longitudinal viscosities at frequency s, ρ is the solvent density, and C_s is the sound velocity in the solvent. The viscosities are related by

$$\eta_1(s) = 4/3\eta_s(s) + \eta_v(s), \tag{8}$$

where $\eta_v(s)$ is the frequency dependent volume viscosity.

A model for the frequency dependence of the solvent shear and volume viscosities must now also be adopted. The model must reflect the fact that not all the solvent motions contributing to the zero frequency viscosities will contribute to the high frequency viscoelastic properties. We anticipate that the frequency dependence will generally be complicated, since it will contain contributions from several different solvent motions, such as conformational, rotational, and translational motions. In keeping with previous work, we have adopted a very simple model which attributes all the frequency dependency of the shear and volume viscosities to translational structural relaxation,

$$\eta_s(s) = \eta_s(0)/(1 + s\tau_s), \tag{9a}$$

$$\eta_v(s) = \eta_v(0)/(1 + s\tau_v), \tag{9b}$$

where τ_s and τ_v are structural relaxation times given by[6]

$$\tau_s = \eta_s(0)/G_\infty, \tag{10a}$$

$$\tau_v = \eta_v(0)/K_r, \tag{10b}$$

where G_∞ is the infinite frequency shear modulus of the solvent and K_r is the relaxation part of the solvent bulk modulus. Equations (7) to (10) have been used in the previous comparisons of the frequency dependent friction model with experimental photoisomerization data.[6,23]

C. Form of the potential surface

The Kramers and frequency dependent friction models contain the assumption that the potential surface is harmonic in the well and barrier regions. Here we consider in more detail a form of the S_1 potential surface which satisfies these assumptions.

The S_1 potential surface of 1,1′-BN is taken to be a piecewise parabolic double well,

$$V(\theta) = \begin{cases} \Delta E + 1/4I\omega_1^2(\theta - \theta_1)^2, & \theta < \phi_1, \quad (11a) \\ (Q + \Delta E) - 1/4I\omega'^2\theta^2, & \phi_1 < \theta < \phi_2, \quad (11b) \\ 1/4I\omega_2^2(\theta - \theta_2)^2, & \theta > \phi_2, \quad (11c) \end{cases}$$

where ω_1 and ω_2 are the well frequencies of conformer 1 and conformer 2, respectively, θ_1 and θ_2 are the dihedral angles characterizing these conformers, ΔE is the energy difference between the two minima, and ϕ_1 and ϕ_2 are the locations of the joins of the three parabolic segements. The form of the potential specified in Eq. (11) is shown in Fig. 2. The requirement that the potential and its first derivative be continuous over the entire range of θ provides a set of equations which specify the joins ϕ_1 and ϕ_2, and which give relationships between the three frequencies. These relationships are

$$\omega_1^2\omega'^2/(\omega_1^2 + \omega'^2) = 2Q/I\theta_1^2 \tag{12a}$$

and

$$\omega_2^2\omega'^2/(\omega_2^2 + \omega'^2) = 2(Q + \Delta E)/I\theta_2^2. \tag{12b}$$

The rate expressions, Eqs. (1) and (5), are strictly only applicable to the escape from a single well potential. However, for the friction range for which Eqs. (1) and (5) are valid the double well nature of the potential considered here has no effect and these equations are still applicable.[13] Since we will be considering the barrier crossing from conformer 1 to conformer 2, the frequency ω appearing in Eqs. (1) and (5) is actually the frequency of the higher energy well, ω_1. Thus the rate expressions involve three potential parameters: ω_1, ω', and Q. For 1,1′-BN the well frequency ω_1 can be evaluated from independent spectroscopic data, since it is related to the frequency of torsional oscillations of excited conformer 1, by $\bar{\nu}_1 = \omega_1/2\pi c$. This torsional mode was recently observed in the fluorescence excitation spectrum of 1,1′-BN in a supersonic jet and had a frequency of 30 cm^{-1},[39] which gives $\omega_1 = 5.7$ ps^{-1}. This value will be used through this paper. Note that since ω_1 is known, Eq. (12a) allows another independent potential parameter to be eliminated, since it provides a unique relationship between ω' and Q. By substituting the values $I = 9.82 \times 10^{-45}$ kg m^2, determined from the x-ray structural data for 1,1′-BN,[40] $\omega_1 = 5.7$ ps^{-1}, and

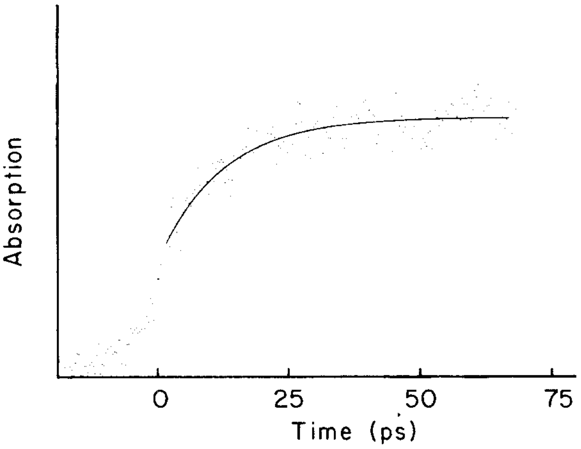

FIG. 4. Induced transient absorption vs probe pulse delay time for a 5×10^{-3} M solution of 1,1'-binaphthyl in ethanol. The points are experimental data and the solid line is the best fit of Eq. (14) with $c = 0.5$ and $\tau = 12.2$ ps.

$\theta_1 = 20°$, this relationship can be written in a more useful form,

$$\omega'^2 = 1072q/(32.5 - 33q), \tag{13}$$

where $q = Q/(500\ \mathrm{cm}^{-})$ is a dimensionless barrier height and ω' is expressed in units of ps^{-1}. Thus the only *independent* potential parameter appearing in the rate expressions is the barrier height Q. This reduction in the number of independent parameters will be important later since it will allow a more reliable comparison to be made between the theoretical rate expressions and the experimental rate data.

IV. RESULTS AND DISCUSSION

A. Data analysis

A set of data for 1,1'-BN in ethanol is shown in Fig. 4. These data show the change in absorption at 600 nm as a function of time following excitation at 300 nm. A fast and a slow rise of absorption are evident, which was observed in all the solvents we studied. The fast rise time was shorter than the instrumental response time (~5 ps, the convolution of pump and probe pulses) and was not resolved in any of the solvents. In the earlier study of 1,1'-BN, a 2.5 ps fast rise time in each of the three solvents was observed.[1] The fast rise time is apparently independent of solvent viscosity, which strongly implies that it is not related to the exciting state conformational change. The origin of this rapidly appearing transient absorption is unknown at present.

The slow rise time component of the transient absorption was dependent on solvent viscosity. It is believed to arise from those molecules which are excited into the higher energy well in the S_1 potential and subsequently undergo the conformational change to reach the lower energy well.[1] This explanation is consistent with the transient absorption spectra of 1,1'-BN,[26] which show that the transient absorption at 600 nm is predominantly due to molecules in the lower energy well. The rise time of the slow component of the transient absorption therefore provides the rate of barrier crossing on the S_1 surface. In analyzing our transient absorption data we have only considered the slow rise component, which we fit with the following equation:

$$A(t) = a(1 - ce^{-t/\tau}), \tag{14}$$

where $A(t)$ is the probe absorption at delay time t, a is an empirical amplitude parameter, c is the fraction of the amplitude due to the slow rise component, and τ is the slow rise time. This equation is an approximation to the true two component rise, valid for times after the fast rise is complete. The influence of overall reorientation of 1,1'-BN on the transient absorption kinetics can be ignored since the reorientation times are considerably longer than the slow rise time.[1] Equation (14) was fitted to the slow rise by adjusting a, c, and τ according to an nonlinear least squares algorithm.[41] The fit to the data in Fig. 4 is shown by the solid line. Excellent fits were obtained in all cases.

The fraction c of the slow component in the two component rise was found to be $c = 0.5 \pm 0.1$ in all the solvents, indicating that the long-time absorptions due to the fast and slow rise components were equal. This is in accord with the earlier study[1] where it was found that the long time absorption when the pump and probe polarization directions were parallel, a situation where the slow rise component was of negligible amplitude, was one half that for orthogonal polarizations. The slow rise times determined from the fitting procedure are presented in Table I for each of the solvents used in this study. The slow rise time in *n*-heptanol was also measured in the earlier study—a value of 22 ± 4 ps at 20 °C was reported.[1] This agrees well with our value, although better agreement is obtained when the slight temperature difference is considered. The results for the other solvents in Table I have not been previously reported.

The inverse of the slow rise time we take to be the barrier crossing rate from the higher to the lower energy well. The reverse crossing process by equilibrated species in the lower well need not be considered since the energy difference between the two energy minima is estimated to be 1050 cm^{-1}.[25] The reverse crossing will thus be slower by a factor of ~200 and will not contribute on the picosecond time scale. The barrier crossing rate is shown as a function of the solvent shear viscosity (zero frequency viscosity) in Fig. 5.

B. Comparison with theoretical models

The data of Fig. 5 were first compared with the Kramers model, Eq. (1). The friction coefficient was calculated from

TABLE I. Experimental rise times and theoretical comparisons. The experimental rise time τ determined from the best fit of Eq. (14) to the slow rise component of the transient absorption for each solvent and the theoretical rise times calculated from the best fit to the data for the Kramers model are shown.

Solvent	Viscosity (cP)	Expt (ps)	Kramers[a] (ps)
Ethanol	1.08	12.2 ± 1.0	12.2
n-Propanol	2.23	13.7 ± 1.0	13.9
n-Butanol	2.95	15.0 ± 1.0	15.2
n-Pentanol	4.33	17.6 ± 1.0	17.7
n-Hexanol	5.27	19.2 ± 1.0	19.5
n-Heptanol	6.90	24.0 ± 2.0	22.9
n-Octanol	8.95	27.0 ± 2.0	27.4

[a] Two parameter fit: $Q = 460\ \mathrm{cm}^{-1}$, $d = 2.8$ Å.

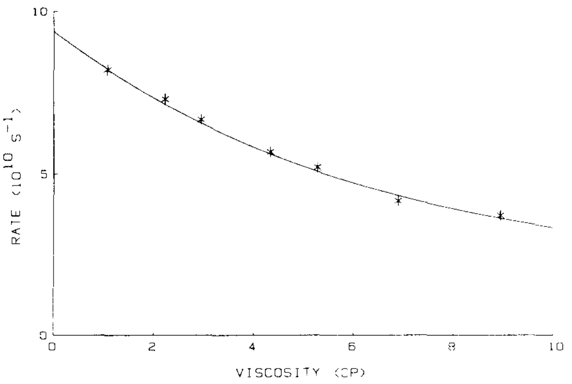

FIG. 5. Barrier crossing rate vs solvent shear viscosity. The stars are experimental data. The line is the best fit of Kramers equation, Eq. (1). See the text for details.

Eqs. (2) and (3) using $r = 1.21$ Å and $I = 9.82 \times 10^{-45}$ kg m^2, which were calculated from the x-ray structural data.[40] The use of Eq. (13) and $\omega_1 = 5.7$ ps^{-1} left the barrier height Q as the only known potential parameter: it was estimated to lie in the range 140–480 cm^{-1}.[25] In view of this uncertainty Q was taken to be an adjustable parameter to be determined by fitting Eq. (1) to the data of Fig. 5. The spherical radius d was also taken to be an adjustable parameter to account for possible deviation from spherical shape and slip boundary condition. Equation (1) was fitted to the data by adjusting these two parameters according to a nonlinear least squares algorithm.[41]

The best fit of Kramers equation is shown by the line in Fig. 5. Rise times for each of the solvents calculated from this best fit are also included in Table I. The value of the parameters used to obtain this fit are $Q = 460 \pm 20$ cm^{-1} and $d = 2.8 \pm 0.2$ Å. The fit is excellent over the entire viscosity range and the barrier height is within the expected range. In fact, this value for the barrier height is precisely equal to that obtained by attributing the difference in the low temperature fluorescence origins of naphthalene and 1,1′-BN entirely to excited state energy differences[25]—that is, by assuming that the naphthyl–naphthyl interaction energy in the ground state equilibrium conformation is small compared to that in the excited state. The value for the radius is in excellent agreement with the steric radius of 3.0 Å calculated from the molecular volume of a naphthyl group,[42] A result which strongly supports the use of Eqs. (2) and (3) to evaluate the friction coefficient. It is also interesting to note that the translational diffusion coefficient calculated from slip hydrodynamics for a 3.0 Å sphere agrees well with the measured diffusion coefficient of naphthalene in solution.[45] Our results thus indicate that the hydrodynamic radius of a naphthalene molecule are equal, within experimental error, which implies that hydrodynamics interactions between the naphthyl groups in 1,1′-BN are not important.[9]

The three barrier crossing rates measured in the earlier study of 1,1′-BN[1] have previously been compared with Kramers equation using a two parameter fitting procedure similar to that used here.[9] A good fit was obtained using the parameter $Q = 475$ cm^{-1} and $d = 1.8$Å. This estimate of the barrier height is in agreement with the value found here but the radius is considerably smaller than our value. The difference is presumably due to differences in the parametrization schemes. In our scheme the spectroscopically determined value of ω_1 was used, which enabled Eq. (12a) to be solved to provide a relationship between ω_1 and Q. No knowledge of the lower energy well was required. At the time of the earlier comparison,[9] ω_1 was unknown and a value for ω_2 had to be chosen to enable Eqs. (12a) and (12b) to be solved to give ω_1 and ω' as functions of Q.[9] The results obtained by this procedure will obviously depend on the choice of ω_2. It should be noted, however, that values for Q and d which are very similar to those found in the previous analysis[9] are retrieved when our data are analyzed in the same way. For Eqs. (12a) and (12b) we find $\omega' = 21.5$ ps^{-1} and $\omega_2 = 11.3$ ps^{-1} using $Q = 460$ cm^{-1}. The potential surface shown in Fig. 2 was actually calculated using these values and appears to be consistent with our knowledge of the potential surface.

It is of interest to determine whether our results fall in the Smoluchowski limit of the Kramers model. In Fig. 6 the barrier crossing rate is shown as a function of the inverse of the solvent shear viscosity. The rate calculated from the Smoluchowski equation, Eq. (4), using the best fit values of Q as determined above, is also shown. It is apparent that the data do not lie in the Smoluchowski limit, although the limit was being approached in the highest viscosity solvent. This is consistent with the condition for the validity of the Smoluchowski equation given in Sec. III A.

The excellent fit of our data to the Kramers theory using zero frequency friction (static value) suggests that the isomerization can be described as a Markovian process. For such a process the treatment of Grote–Hynes reduces to that of Kramers and would therefore give the same excellent fit to our data. Despite this agreement between experiment and the Kramers model, it is of interest to observe that at the high frequency of the barrier, $\omega' = 2 \times 10^{13}$ s^{-1} one might have expected non-Markovian effects to be important. This is based on the suggestion[3,23] that for barriers of sufficiently

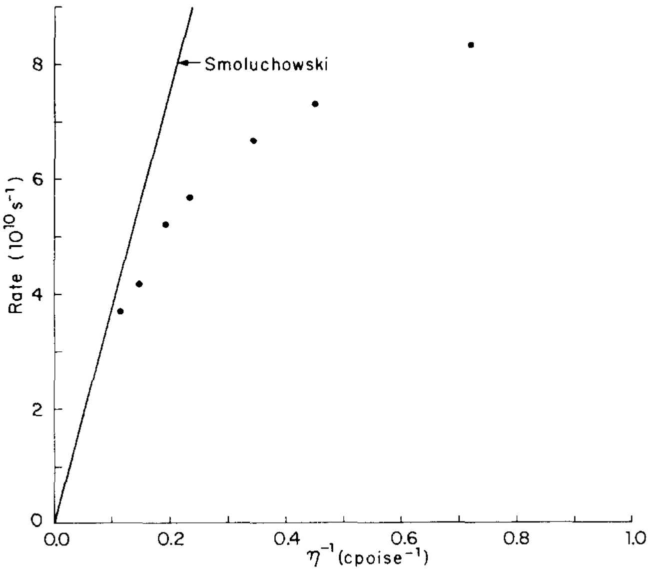

FIG. 6. Barrier crossing rate vs the reciprocal of the solvent shear viscosity. The points are experimental data and the solid line is calculated from the Smoluchowski equation. See the text for details.

high frequency, $10^{12}-10^{13}$ s^{-1}, that the effective friction acting on the conformational coordinate is different from the zero-frequency friction. In other words, the relaxation of the solvent motions is not sufficiently rapid relative to the motion of the molecule along the reaction coordinate in the vicinity of the barrier, where the forces are changing rapidly (high ω'), to describe the fluctuating forces as uncorrelated and thus permit the use of the zero frequency friction. Although the values of the hydrodynamic radius and the barrier height used to fit our kinetic data to the Kramers model are reasonable we cannot exclude the possibility that they are compensating for a reduced friction arising from non-Markovian effects.

For these reasons we sought to determine if we could also obtain a reasonable fit of our data to a non-Markovian treatment such as that of Grote–Hynes as outlined in Sec. III. To effect this comparison we note again that we must superimpose on the Grote–Hynes model a model of the frequency dependent friction. The one we use is a frequency dependent hydrodynamic friction for a sphere. To obtain the frequency dependent friction, Eq. (7), the values of $\eta_s(0)$, ρ, and C_s were taken from standard tables.[43] The volume viscosity $\eta_v(0)$ was calculated from Eq. (9) using values of the longitudinal viscosity $\eta_l(0)$ evaluated from ultrasonic absorption data.[43] The relaxation part of the solvent bulk modulus is given by $K_r = K_0 - K_\infty$, where $K_0 = \rho C_S^2$. The properties of the solvents at infinite frequency should be similar to those of the solvents in their glassy state, where reorientation and translation are frozen out. We have therefore used the value $G_\infty = 1.5\times 10^9$ N m^{-2} and the ratio $G_\infty/K_\infty = 0.26$, which are characteristic of organic glasses.[44]

Equation (5) could then be fitted to the rate data, in conjunction with Eq. (13), by adjusting Q and d, as was done for the Kramers fit. However, no value of Q could be found which provided a reasonable fit to the data. In fact, for all Q values in the expected range, Eq. (5) predicted barrier crossing rates which showed essentially no change from solvent to solvent. The reason for this appeared to be that Eq. (6), lead to values of the reactive frequency lying in the high frequency limit of Eq. (7), where $\zeta_r(s)$ goes to a constant limiting value. The tendency of the hydrodynamic friction of Eq. (7) to reach a limiting value at high frequency is an unphysical behavior.[35–38] In fact, the high frequency or very short-time behavior of the friction is expected to be dominated by solvent–solvent binary collisions, rather than by collective hydrodynamic behavior, in which case the friction should approach zero at very high frequencies. It thus appears that we are unable to test whether the isomerization dynamics can be fitted to the non-Markovian model of Grote–Hynes due to a breakdown in the applicability of the hydrodynamic frequency dependent friction model at high frequencies. It is perhaps relevant to observe that the optimal, though as pointed out not good, fit of the photoisomerization kinetics of *trans*-stilbene[6] to the Grote–Hynes formulation, using a hydrodynamic treatment of the frequency-dependent friction yields the values $\omega' = 1.5$ ps^{-1} and $\omega_1 = 96$ ps^{-1}. The barrier frequency would thus be considerably lower than the reactant well frequency, remarkably flat, and as noted[6] is probably an unphysical, i.e., incorrect potential surface for the motion. It is possible that the breakdown of the hydrodynamic model at high frequencies imposes a requirement that the reactive frequencies not fall in the high frequency limit in order to obtain a fit with the isomerization data.

We have pursued this point by allowing ω' to vary in addition to Q and d. This permits us to explore what type of three parameter fit would be possible in a theory containing a hydrodynamic frequency dependent friction as given by Eq. (7), noting that a two parameter fit did not fit our data. Allowing ω' to vary independently of Q corresponds to abandoning the assumption of a piecewise parabolic potential surface, an assumption used in the Kramers treatment. The values used to obtain a fit were $Q = 350 \pm 30$ cm^{-1}, $\omega' = 2.73 \pm 0.05$ ps^{-1}, and $d = 3.0 \pm 0.3$ Å. This three parameter fit, though not as good as the Kramers two parameter fit, yields reasonable values for d and Q but gives a considerably smaller barrier frequency ω'. In fact it is now smaller than the reactant well frequency, a result that we have noted was also found to be the case for *trans*-stilbene. We speculate that the small values obtained for ω' in *trans*-stilbene and 1,1′-binaphthyl are more likely a consequence of the unphysical behavior of Eq. (7) at high frequency and reflects the attempt to fit the kinetic data using Eq. (7), rather than to an actual feature of the potential surfaces. Given the present lack of knowledge of the high frequency behavior of the friction, including uncertainties in the values of G_∞ and K_r, we believe it is not possible to achieve a definitive comparison with a non-Markovian model such as that of Grote–Hynes.

The important finding in this work is the success of the Kramers model in reproducing the experimental data using reasonable parameter values. It is interesting to compare our results with those reported in the photoisomerization studies of other systems. The viscosity dependence of the photoisomerization rate measured for diphenylbutadiene,[2] *trans*-stilbene,[6] and DODCI[3] showed substantial deviation from Kramers equation over the same viscosity range as used in this study. In these molecules it is likely that the isomerization involves more than a single structural coordinate and thus would have different frictional properties along these different coordinates. However, in 1,1′-BN, where the data are in excellent agreement with Kramers equation, the assumption that the conformational change involves only a single coordinate, the dihedral angle, is more reasonable. Thus our results are consistent with the idea that deviations from Kramers behavior can be due to breakdown[3,6] of the one-dimensional assumption implicit in the Kramers approach and not necessarily to a breakdown in the assumption that the friction is frequency independent in accord with a Markovian process. Of course, the results for a single molecule cannot constitute a proof of this possibility and it will be interesting to pursue these studies with a variety of other systems. Our results do show, however, that deviation from Kramers behavior is not a universal phenomenon in the conformational dynamics of flexible molecules in solution.

V. CONCLUSIONS

The viscosity dependence of the conformational dynamics of 1,1′-BN in alcohol solutions can be understood within the framework of the strong coupling limit of the frictional barrier crossing model. Excellent agreement with experiment is obtained for the Kramers version of the model, which treats the friction as Markovian. This is the first experimental support of the Kramers model which extends over the entire frictional regime for which the assumptions of the theory are valid, i.e., from intermediate friction values where the rate is described by the Kramers equation, to the very high friction limit where the Kramers equation reduces to the Smoluchowski limit. It is, however, interesting to note that despite the high barrier frequency in 1,1'-BN, non-Markovian effects are absent; a conclusion deserving further study.

ACKNOWLEDGMENTS

The authors wish to gratefully acknowledge the National Science Foundation, The Air Force Office of Scientific Research, and the Joint Services Electronics Programs 29-82-K-0080 for their support, and also to thank Professor B. J. Berne, Professor J. L. Skinner, and Professor B. Alder for helpful discussions.

[1] C. V. Shank, E. P. Ippen, O. Teschke, and K. B. Eisenthal, J. Chem. Phys. **67**, 5547 (1978).
[2] S. P. Velsko and G. R. Fleming, J. Chem. Phys. **76**, 3553 (1982).
[3] S. P. Velsko, D. H. Waldeck, and G. R. Fleming, J. Chem. Phys. **78**, 249 (1983).
[4] K. M. Keery and G. R. Fleming, Chem. Phys. Lett. **93**, 322 (1983).
[5] R. Hochstrasser, Pure Appl. Chem. **52**, 2683 (1980).
[6] G. Rothenberger, D. K. Negus, and R. M. Hochstrasser, J. Chem. Phys. **79**, 5360 (1983).
[7] V. Sundstrom and T. Gillbro, Chem. Phys. Lett. **109**, 538 (1984).
[8] D. L. Hasha, T. Eguchi, and J. Jonas, J. Chem. Phys. **75**, 1571 (1981); J. Am. Chem. Soc. **104**, 2290 (1982).
[9] J. S. McCaskill and R. G. Gilbert, Chem. Phys. **44**, 389 (1979).
[10] R. S. Larson and M. D. Kostin, J. Chem. Phys. **72**, 1392 (1980).
[11] P. B. Visscher, Phys. Rev. B **13**, 3272 (1976); **14**, 347 (1976).
[12] R. F. Grote and J. T. Hynes, J. Chem. Phys. **73**, 2715 (1980).
[13] B. Carmelli and A. Nitzan, J. Chem. Phys. **80**, 3569 (1984).
[14] R. F. Grote and J. T. Hynes, J. Chem. Phys. **74**, 4465 (1981).
[15] G. van der Zwan and J. T. Hynes, J. Chem. Phys. **77**, 1295 (1982).
[16] B. Carmelli and A. Nitzan, Phys. Rev. Lett. **51**, 233 (1983).
[17] P. L. Bhatnager, E. P. Gross, and M. Krook, Phys. Rev. **94**, 511 (1954).
[18] J. L. Skinner and P. G. Wolynes, J. Chem. Phys. **69**, 2143 (1978); **72**, 4913 (1980).
[19] B. J. Berne, J. L. Skinner, and P. G. Wolynes, J. Chem. Phys. **73**, 4314 (1980).
[20] D. K. Garrity and J. L. Skinner, Chem. Phys. Lett. **95**, 46 (1983).
[21] R. O. Rosenberg, B. J. Berne, and D. Chandler, Chem. Phys. Lett. **75**, 162 (1980); J. A. Montgomery, Jr., D. Chandler, and B. J. Berne, J. Chem. Phys. **70**, 4056 (1979).
[22] H. A. Kramers, Physica **7**, 284 (1940).
[23] B. Bagchi and D. W. Oxtoby, J. Chem. Phys. **78**, 2735 (1983).
[24] R. A. Friedel, M. Orchin, and L. Reggel, J. Am. Chem. Soc. **70**, 199 (1948).
[25] R. M. Hochstrasser, Can. J. Chem. **39**, 459 (1961).
[26] M. F. M. Post, J. Langelaar, and J. D. W. van Voorst, Chem. Phys. Lett. **32**, 59 (1975).
[27] M. J. Riley, A. R. Lacey, M. G. Sceats, and R. G. Gilbert, Chem. Phys. **72**, 83 (1982).
[28] R. W. Bigelow and R. W. Anderson, Chem. Phys. Lett. **58**, 114 (1978).
[29] M. F. M. Post, J. K. Eweg, J. Langelaar, J. D. W. van Voorst, and G. ter Maten, Chem. Phys. **14**, 165 (1976).
[30] D. P. Millar and A. H. Zewail, Chem. Phys. **72**, 381 (1982).
[31] P. Bado, S. B. Wilson, and K. R. Wilson, Rev. Sci. Instrum. **53**, 706 (1982).
[32] J. Happel and H. Brenner, *Low Reynolds Number Hydrodynamics* (Prentice Hall, Englewood Cliffs, 1965).
[33] G. R. Fleming, A. E. W. Knight, J. M. Morris, R. J. Robbins, and G. W. Robinson, Chem. Phys. Lett. **51**, 399 (1977).
[34] D. Kivelson, Faraday Symp. **11**, 7 (1977).
[35] R. Zwanzig and M. Bixon, Phys. Rev. A **2**, 2005 (1970).
[36] H. Metiu, D. W. Oxtoby, and K. F. Freed, Phys. Rev. A **15**, 361 (1977).
[37] R. F. Grote, G. van der Zwan, and J. T. Hynes, J. Chem. Phys. **88**, 4676 (1984).
[38] D. Levesque and L. Verlet, Phys. Rev. A **2**, 2514 (1970).
[39] H. T. Jonkman and D. A. Wiersma, Chem. Phys. Lett. **97**, 261 (1983).
[40] K. A. Kerr and J. M. Robertson, J. Chem. Phys. **13**, 1146 (1969); R. B. Kress, E. N. Duesler, M. C. Etter, I. C. Paul, and D. Y. Curtin, J. Am. Chem. Soc. **102**, 7709 (1980).
[41] P. R. Bevington, *Data Reduction and Error Analysis in the Physical Sciences* (McGraw–Hill, New York, 1969).
[42] J. T. Edwards, J. Chem. Ed. **47**, 261 (1970).
[43] *Landolt-Bornstein*, edited by K. H. Hellwege and A. M. Hellwege (Springer, Berlin, 1967), Group II, Vol. 5.
[44] T. Fox and F. Flory, J. Am. Chem. Soc. **70**, 23 (1948); J. Appl. Phys. **21**, 581 (1950); J. Chem. Phys. **55**, 221 (1951); J. Polym. Sci. **14**, 315 (1954).
[45] L. G. Longworth, J. Colloid Interface Sci. **22**, 3 (1966).